ELSEVIER

Earth and Planetary Science Letters 206 (2003) 1–14

EPSL Frontiers

www.elsevier.com/locate/epsl

Frontiers

# Apatite (U–Th)/He thermochronometry: methods and applications to problems in tectonic and surface processes

Todd A. Ehlers *, Kenneth A. Farley

*California Institute of Technology, Division of Geological and Planetary Sciences, MC 100-23, Pasadena, CA 91125, USA*

Received 11 July 2002; received in revised form 1 October 2002; accepted 5 November 2002

**Abstract**

In the last decade apatite (U–Th)/He thermochronometry has emerged as an important tool for quantifying the cooling history of rocks as they pass through the upper 1–3 km of the crust. The low closure temperature of this technique (~70°C) has gained the interest of geomorphologists and tectonocists because it is applicable to interdisciplinary studies in landform evolution, structural geology, and geodynamics. We discuss current analytical techniques, the temperature calibration of the method, and sample quality considerations. Results from 1D, 2D and 3D thermo-kinematic numerical models are used to illustrate applications of He thermochronometry to problems in tectonics and landform evolution.


*Keywords:* apatite; (U–Th)/He; thermochronometry; surface processes; tectonics; numerical modeling

## 1. Introduction

A recent resurgence of interest in dating minerals via $^4$He ingrowth has been driven by an improved understanding of the behavior of He in minerals [1–4], development of robust analytical techniques [3,5], and demonstration that important geologic questions are uniquely accessible with He dating [6–8]. So far only fluorapatite, $Ca_5(PO_4)_3(F,Cl)$, has been widely studied for He chronometry. The focus on apatite arises from its ubiquity and moderately high U and Th content, but more importantly because He accumulation in apatite occurs only at temperatures below ~70–75°C [9]. At higher temperatures diffusion removes He as fast as it is produced by decay. As a consequence apatite (U–Th)/He ages document the latest stages of cooling in the uppermost crust, at even lower temperatures than the apatite fission track method (~100°C closure) [10].

As with apatite fission track dating, apatite He dating has been used to study tectonic processes that cause rock cooling. For example, normal faulting causes rocks in the footwall to experience enhanced and recent cooling relative to the hanging wall, which is recorded as younger He ages in the footwall (Fig. 1). Under favorable circumstances the He age distribution can be used to deduce

* Corresponding author. Department of Geological Sciences, University of Michigan, 2534 C.C. Little Building, 425 East University, Ann Arbor, MI 48109-1063, USA..
*E-mail addresses:* tehlers@umich.edu (T.A. Ehlers), farley@gps.caltech.edu (K.A. Farley).

0012-821X/02/$ – see front matter 
PII: S0012-821X(02)01069-5

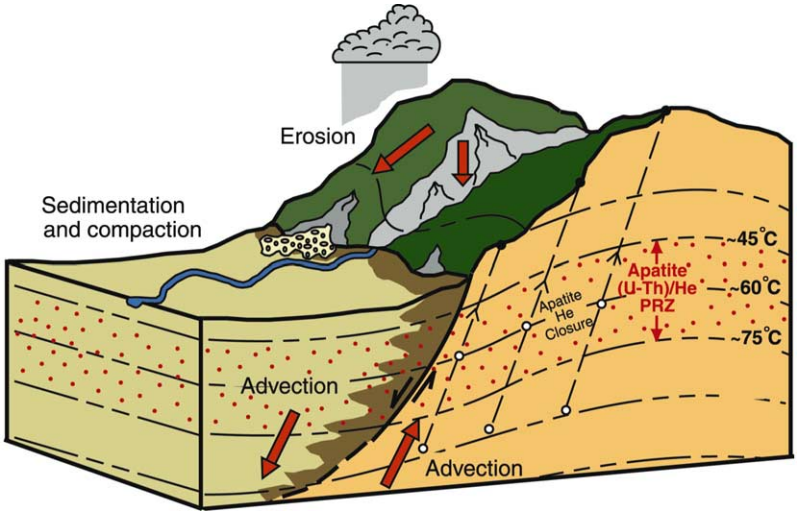


Fig. 1. Thermal processes in a normal-fault bounded range that influence the interpretation of apatite (U–Th)/He data. Isotherms (dashed lines) are curved from advection of mass and heat (red arrows) in the footwall and hanging wall, and by topographic relief. Rocks in the subsurface (open circles) are exhumed and sampled at the surface (filled circles). The stippled red zone between ~45 and ~75°C represents the helium partial retention zone (HePRZ) where helium diffusion is neither fast enough to maintain a zero concentration, nor slow enough for complete retention of helium. Modified from [11].

the timing, rate, and extent of motion on the fault [7,11]. The lower closure temperature of the apatite He system makes it possible to detect and quantify degrees of tectonically induced cooling that are too small to be recorded by higher temperature systems. Additionally, for very young or rapid cooling events the He method offers better precision. Other tectonic problems can be addressed by pairing apatite He ages with those from higher temperature systems to better document the last few hundred degrees of rock cooling [12,13]. Thus apatite He ages can supplement and in some cases replace other dating techniques in a range of tectonic studies.

Apatite He ages are strongly influenced by perturbations in the thermal field of the shallow crust. Most notably, crustal isotherms mimic surface topography, with the relief on isotherms becoming increasingly significant closer to the surface (e.g. Fig. 1). The lower the closure temperature of the system, the greater the influence of topography on cooling ages. Although the potential for topography to confound cooling age patterns has been recognized [14,15], the sensitivity of apatite He ages is such that they can be used to infer the existence and even the evolution of topography in the past [6]. Of course this topography may be produced by faulting (Fig. 1), so tectonic interpretations of apatite He ages cannot be made in isolation from the effects of surface topography. This interplay underscores the need for quantitative models that link the thermal effects of tectonics with surface processes such as relief development, river incision and glacial erosion which ultimately control the time–temperature history of rocks in the uppermost crust as well as the long-term evolution of the landscape. In this regard apatite He ages may provide an important tool for linking geomorphology, which relies largely on analyses of modern topography and recent surface processes, with longer time scale effects documented by structural geology.

In this paper we discuss the principles, techniques and limitations of the apatite He dating method and illustrate the use of He ages to investigate tectonic and geomorphologic processes. We emphasize general concepts over specific details and applications, which have been reviewed in other papers (e.g. [5]).

## 2. The apatite He dating method

### 2.1. Background and analytical methods

(U–Th)/He dating is based on the ingrowth of α particles produced by U and Th series decay. In time $t$ the amount of helium produced in a mineral is $^4He = 8^{238}U(e^{\lambda 238t}-1)+7/137.88^{238}U(e^{\lambda 235t}-1)+6^{232}Th(e^{\lambda 232t}-1)$. Measurements of parent and daughter isotopes define the time since closure assuming no extraneous sources of He. With the exception of inclusions of other minerals (see below) and, less commonly, of fluid [2,16], this is a good assumption [5]. There are no fundamental limitations on the range of accessible ages; He ages as young as a few hundred kyr (on volcanic apatites [17]) and as old as 4.56 Ga (on a meteorite [18]) have been reported. However, for samples with crystallization ages of $< \sim 1$ Ma secular disequilibrium in the $^{238}U$ series modifies the form of the age equation [17].

The most widely adopted procedure for apatite He dating involves in vacuo extraction of He by heating in a furnace [1–3] or with a laser (e.g. [20,21]) followed by purification and analysis by mass spectrometry. After removal from the vacuum system, the apatites are dissolved and U and Th analyzed, usually by inductively coupled plasma mass spectrometry (ICP-MS). For apatites of typical U, Th, and He content the analytical precision of a He age is usually better than 1.5% (2σ) and accuracy better than 1% [5]. Using low-blank laser extraction it is possible to date single apatites with no substantial loss of precision. In practice, apatite He ages do not reproduce this well.

Mineral inclusions with high U and Th concentrations, especially zircon and monazite (Fig. 2), produce erroneously high He ages in some apatites [22,23]. Microscopic examination of grains to be dated greatly reduces this problem [5]. However, some inclusions may be too small to detect (Fig. 2e). Other techniques for recognizing analyses compromised by inclusions have been developed [5]. Most importantly, inclusions tend to be heterogeneously distributed from grain to grain, causing poor age reproducibility. Thus age reproducibility is an indispensable demonstration of the quality of an apatite He age.

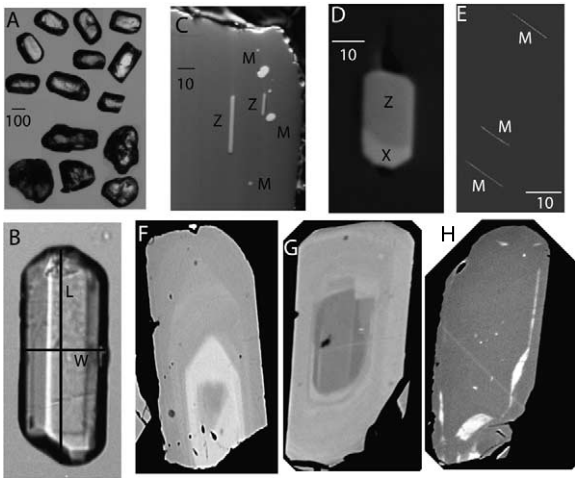


Fig. 2. Photomicrographs of apatite crystals. (A) This panel shows euhedral grains which have typical morphology appropriate for α-ejection correction (upper), and anhedral and rounded grains with geometries too complex to apply a straightforward correction (lower). (B) A typical euhedral crystal appropriate for α-ejection correction, with the grain length ($L$) and prism cross-section ($W$) indicated. (C–E) These three SEM electron backscatter images show common inclusions in apatite that can yield erroneously high He ages: **M**onazite, **Z**ircon, and **X**enotime. The inclusions in C and D are large enough to be easily detected in unpolished grains under a binocular microscope, but the small needles of monazite in E are not easily detected. (F–H) These SEM backscatter images show zonation of major and minor elements (mostly Y, Ce, La, Si, and P). Bright regions are enriched in Y, Ce, and La, and ICP-MS analyses show that these elements correlate strongly with U and Th in these apatites. Thus these images are indicative of zonation in U and Th. Note that normal, reversed and irregular zonation can occur and each will have a different and potentially large effect on He ages. In panels A and C–E, scale bar is in μm; in panels B and F–H the apatite grains are ∼300 μm long.

### 2.2. α Ejection

U and Th emit α particles which travel ∼20 μm through apatite. As a result, α particles may be ejected from crystal edges or injected from surrounding grains (Fig. 3, inset). If not corrected for, α transport can cause errors of up to tens of % in He ages [24]. Although implantation may be significant in unusually U,Th-poor apatites or those with high-radioactivity surroundings [17], in general it can be ignored [24]. Surface-to-volume ratio and the distribution of parent atoms relative to the surface control the magnitude of

α ejection. By assuming idealized geometry and a homogeneous spatial distribution of U and Th, Farley et al. [24] modeled the fraction of αs retained ($F_T$) in crystals of various dimensions. Age determinations at Caltech indicate that most apatites are hexagonal prisms with cross sections between 75 and 170 μm; grains in this size range have $F_T$ values between ~67% and ~85% (Fig. 3). Without correcting for this effect typical apatites would yield He ages that underestimate the time since He closure by ~$(1-F_T)$, or between 15 and 33%.

To account for this effect it is common practice to measure the physical dimensions of a crystal to be dated (Fig. 2b), from which an α-ejection correction is computed [24]. Fig. 3 shows that the factor by which 'raw' He ages must be multiplied to correct for ejection varies from ~1.2 to ~1.5. The general validity of this correction has been confirmed [24]. Fig. 3 also shows a conservative estimate of the uncertainty in the correction. For grains > ~125 μm in cross section, the ±2% uncertainty is comparable to the analytical error in isotope measurements, but this source of age uncertainty grows rapidly as grain size decreases. In general the observed reproducibility of He ages is consistent with the combination of analytical and α ejection uncertainties, or about ±5% (2σ) on reasonably large apatite crystals [8].

The ejection correction assumes a homogeneous spatial distribution of U and Th, which is usually but not always correct (Fig. 2f–h). α Ejection can be computed for zoned crystals [24,25], but since it is not generally possible to date grains in which zonation has already been measured, homogeneity is usually assumed. Ages computed in this way for grains zoned as in Fig. 2 would be incorrect by ±10–25%. In a sample with zoned apatites we usually find that almost every grain is zoned, but the magnitude and even the sense of zonation varies. This implies that the error in α-ejection correction is similarly variable, and like in the case of inclusions, replicate age determinations provide a powerful means for identifying problematic samples. Extreme variability in U and Th concentration or U/Th ratio among replicates is also a telltale sign of this phenomenon. All of the problematic samples shown in Fig. 2 were detected first by unusually poor age reproducibility. A scanning electron microscopy (SEM) scan on a polished grain mount prior to working with a sample can provide a more direct way to identify samples with zonation and inclusions before analysis begins.

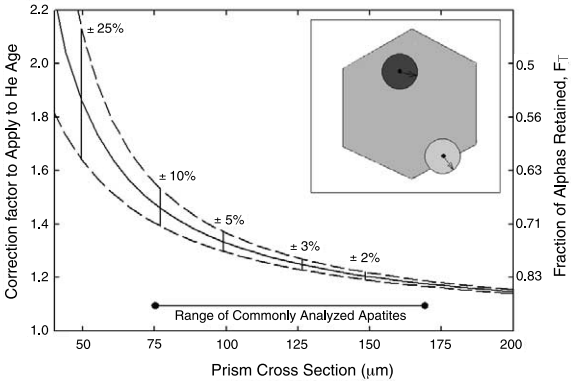


Fig. 3. The consequences of α ejection on apatite He ages. Inset is a conceptual model showing that He atoms will come to rest on the surface of a ~20 μm sphere centered on the parent nucleus. For parent nuclei more than ~20 μm from the edge of the grain (shaded hexagon), all He will be retained (dark circle); for parent nuclei closer to the grain edge some fraction of α particle trajectories will eject the atom from the grain (light circle). In the main figure the curve indicates the approximate factor by which a raw He age must be multiplied to correct for this ejection, assuming a hexagonal prism with a length/cross section ratio of 3 and decay in the $^{238}U$ series, after [24]. The fraction of αs retained, $F_T$, is shown for comparison on the right hand axis. The dashed curves indicate the 1σ uncertainty on the correction factor based on grain measurement uncertainties and a conservative estimate of how well typical apatites approximate the idealized hexagonal prism geometry. Numbers above curve indicate 2σ uncertainties at selected cross sections.

### 2.3. He diffusion

The main application of the apatite (U–Th)/He method has been assessment of cooling histories, which demands accurate, quantitative knowledge of He diffusivity. Laboratory step-heating experiments in which the He loss rate is measured as a function of temperature provide the necessary information. In all apatites studied so far He loss is consistent with thermally activated volume diffusion [1–3,26]. Under simplifying assumptions

these data can be converted into diffusion coefficients [27] and then into kinetic parameters which describe the diffusivity as a function of temperature. The simplest way to describe the kinetic parameters is in terms of closure temperature, $T_c$ [28]. Limited high quality diffusion data indicate modest variability in apatite He $T_c$: 60–75°C assuming a cooling rate of 10°C/Myr. This is the lowest known closure temperature among radiometric dating techniques. Several lines of evidence support this closure temperature estimate in the natural setting [7,26,29]. There is no evidence that $T_c$ varies with apatite chemistry, but it does scale with grain size. For example, from 50 to 150 μm in minimum dimension, $T_c$ increases by ~10°C [4].

Laboratory experiments must be done at temperatures at which measurable He loss occurs in minutes to days, temperatures far higher than those at which He loss occurs over geologic time. Thus the laboratory data must be extrapolated to the lower temperatures of interest in nature, typically by ~100°C and four orders of magnitude in diffusivity. As a consequence, small errors in the measured data can grow to substantial uncertainties in the relevant diffusivity. Even the most detailed diffusion analyses have uncertainties in $T_c$ of ±5°C (2σ), and more typical experiments yield uncertainties nearly twice as large. This is an important consideration for understanding He ages. For example, at a cooling rate of 2°C/Myr, a ±10°C uncertainty range in $T_c$ corresponds to an age span of 10 Ma. The point here is that the dominant uncertainty in geologic applications is not the age determination itself, but rather in the attribution of temperature significance to that age.

The diffusive loss rate of He from an apatite depends not only on the kinetic parameters but also on the He concentration gradient. Because alpha ejection reduces the concentration gradient at the edge of a grain, the He loss rate will be slower than in the absence of ejection [4,25]. This effect typically yields an increase of just a few °C in $T_c$ [4]. Of greater concern is zonation in U and Th. Apatites with high concentrations of U–Th near the rim will lose more He by diffusion than a homogeneous apatite would and hence would yield a younger He age, and vice versa [25]. Unfortunately this error reinforces the error arising from erroneous α-ejection correction for zoned grains. More subtly, the magnitude of the error induced by parent zonation depends on cooling rate: a quickly cooled sample experiences little diffusive loss, while a slowly cooled sample spends substantial time at temperatures where small differences in loss rate propagate into large age differences. This observation drives home a larger point: the slower the cooling rate, the greater the sensitivity of a He age to subtle factors controlling He loss, like zonation, grain size, and variability in kinetic parameters. Indeed, a strong correlation between apatite grain size and He age from a single rock may imply very slow cooling [30].

### 2.4. Appropriate samples

While apatite is a ubiquitous phase, the above considerations restrict what samples can be successfully dated using the He method. Most importantly, α ejection requires the presence of apatites > ~75 μm in minimum dimension and with appropriate morphology for α-ejection modeling (Fig. 2a). Unlike fission track dating, He ages cannot easily be determined on small grains or subhedral, fragmentary, needle-like or rounded apatites. Mineral inclusions and to a lesser extent U and Th zonation can also preclude accurate He dating of some samples. Here we generalize what rock types commonly yield apatites that meet these criteria. Medium to coarse-grained granodiorites and tonalites and mildly metamorphosed equivalents have been studied from many localities. These rocks are the generally preferred lithology because they tend to yield abundant, large, inclusion-free, and euhedral apatite crystals. Alkali granites tend to yield lesser amounts of apatite, often smaller in grain size and sometimes very inclusion-rich. Fine-grained granitoids and most volcanics seldom have sufficiently coarse apatites for dating. Gneisses frequently yield large amounts of apatite, but many samples have inclusions, especially of exsolved monazite (Fig. 2e). In addition, these apatites often have strong variability in U and Th content and may commonly be

zoned. Detrital apatites, especially from coarse-grained sandstones, can be dated [29], but often they are too small or poorly shaped to work with. In many cases detrital apatites have abraded surfaces which make it difficult to inspect for inclusions.

For all of these lithologies between 3 and 10 kg of rock is usually sampled, from which mg quantities of apatite are extracted using standard heavy mineral separation techniques.

## 3. Interpretation of He ages

Apatite He ages record the temperature history experienced by rocks transiting the uppermost ~3 km of the crust, which is often controlled by tectonic processes, by erosion, or by the interplay of the two. Here we demonstrate the response of apatite He ages to various geologic processes in isolation, building from simple one-dimensional (1D) models through two-dimensional (2D) tectonic models and concluding with a three-dimensional (3D) model of He ages in eroding landscapes. The goal is to demonstrate what types of information can be obtained from He ages, and where appropriate we refer to studies that illustrate attempts to obtain such information. For these models we have used a numerical solution to the He production–diffusion equation to compute He ages [31], but for simplicity we often refer to the more intuitive He closure temperature concept.

### 3.1. One-dimensional cooling and age–depth relationship

Apatite He ages document cooling commonly produced by exhumation, i.e. motion of rocks toward the Earth's surface. The relevant questions to be addressed by He dating are: what processes caused exhumation and when and how fast did they operate? These questions are often approached by establishing the He age distribution with increasing crustal depth or paleodepth. Under most circumstances crustal temperatures increase and apatite He ages decrease with depth, but the exact pattern of variability depends on the exhumation history. Here we model the 1D case of He ages that might be observed in rocks of a borehole or cliff face after different assumed exhumation rates (Fig. 4). This approach is implicit in many applications of He dating [7,8,21,32].

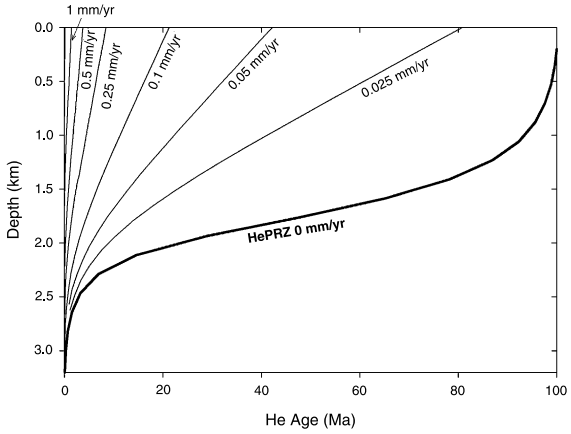


Fig. 4. He ages developed at different exhumation rates assuming a 1D thermal model. The He ages at each depth were determined by first calculating steady-state geotherms for exhumation rates between 0 mm/yr (no exhumation) and 1.0 mm/yr ([15], equations 13 and 23). The cooling history of samples at each depth was recorded and an age was calculated [31]. For the case of a 0 mm/yr exhumation rate the He ages were calculated assuming an isothermal holding time of 100 Myr at each depth. The rapid change in age with depth for this exhumation rate defines the He partial retention zone, HePRZ.

After 100 Myr of isothermal holding, He ages define a characteristic sigmoidal shape (0 mm/yr, Fig. 4). Near the surface predicted ages are old, documenting complete retention of helium. At depths between ~1.5 and ~2.5 km the ages decrease rapidly with depth and are diagnostic of samples located in the helium partial retention zone (HePRZ), where helium diffusion is neither fast enough to maintain a zero concentration, nor slow enough for complete retention of helium [31]. At depths greater than 3 km helium readily diffuses and ages are ~0 Ma.

For rocks experiencing a constant exhumation rate the He age pattern reaches a steady state in which ages increase approximately linearly with depth. The slope of the profile approximates the exhumation rate and is often used to determine the rates of geologic processes (e.g. [15]). Intui-

tively this can be viewed as the successive passage of each point across the closure isotherm; apatites higher in the column crossed this isotherm before rocks deeper in the column. However, the background conductive thermal state is significantly perturbed in regions where exhumation is sufficiently rapid to cause advective heat loss [33]. At higher exhumation rates advection shifts the closure isotherm upward in the crust. In addition, faster cooling increases the closure temperature itself. Therefore the zero age intercept becomes shallower with increasing exhumation rate (Fig. 4).

This discussion assumes a one-dimensional thermal field, but thermo-tectonic processes in real-world settings result in important but often ignored deviations from this assumption (e.g. [12,34]). We illustrate this point by consideration of the thermal field and resulting He ages in normal and thrust fault environments.

### 3.2. Normal fault settings

In normal-fault bounded ranges several processes lead to deviations from a one-dimensional thermal field, including (Fig. 1) [34–37]: (1) lateral heat flow across large, range-bounding faults due to the juxtaposition of a cool hanging wall and a relatively warmer footwall; (2) uplift and erosion of the footwall and sedimentation and burial of the hanging wall; (3) footwall tilt, and (4) topography. These processes can cause significant lateral variations in the apatite He closure temperature depth [34]. Here we explore He age patterns in the footwall of a normal-fault bounded range using a model that includes these phenomena. We assume a steady-state topographic profile and defer consideration of the effects of topography to Section 4.

Fig. 5 shows an example of a 2D numerical model of the thermal field and predicted apatite He ages in the footwall of a major normal fault (the Wasatch Range, Utah). The thermal model assumes a maximum exhumation (footwall) and burial (hanging wall) rate at the fault, a 45° fault dip, and a hinge position of 30 km distance from the fault. The exhumation rate is assumed to decrease linearly across the footwall and hanging wall and is 0 mm/yr beyond the hinge. Samples closest to the fault are exhumed from the greatest depth (10 km) because the exhumation rate is highest there. Predicted isotherm positions are shown in Fig. 5a after 10 Myr of exhumation with a fault-adjacent exhumation rate of 1 mm/yr.

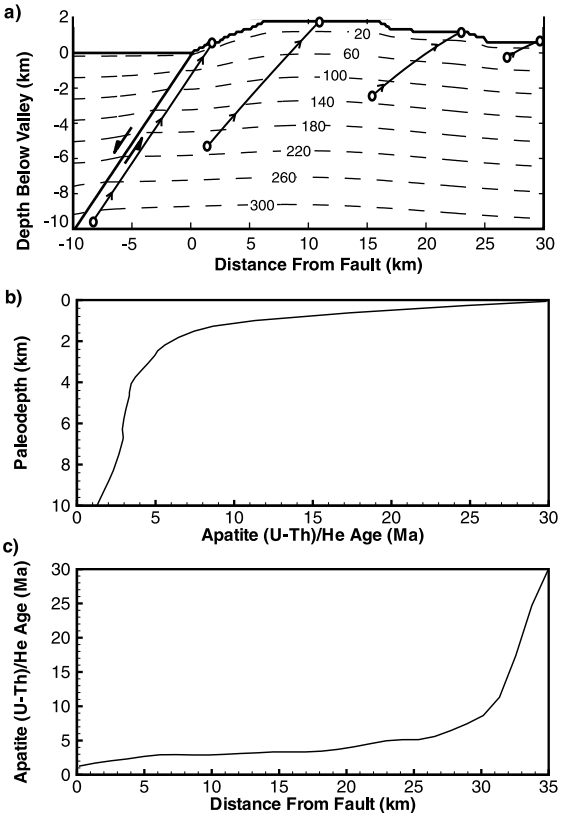


Fig. 5. Thermal field and predicted He ages in the footwall of normal fault (Wasatch Mountains, Utah) after 10 Myr of exhumation. Results were computed using the 2D thermal and He age prediction models of [38] and [11]. (A) Isotherms (dashed lines) are in °C. Open circles with solid lines schematically represent the exhumation trajectory of rock samples at the surface. (B) Predicted He ages versus paleodepth after applying a tilt correction to restore samples to their initial depth. (C) Predicted footwall He ages versus distance from the fault for samples located on the topography.

Isotherms in the footwall are swept upward due to exhumation and topography, and downward in the hanging wall due to sedimentation. This juxtaposition of enhanced and depressed thermal gradients in the footwall and hanging wall, respectively, results in curved isotherms across the

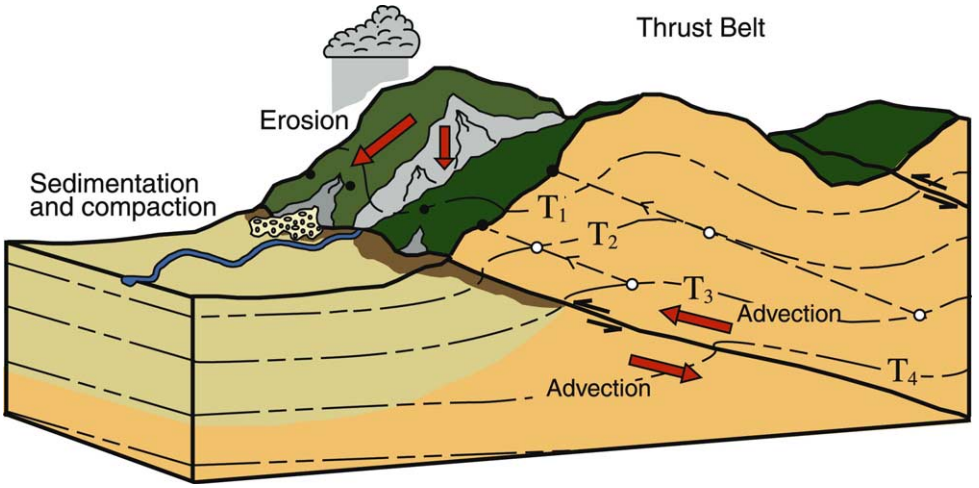


Fig. 6. Thermal processes in a fold and thrust belt that influence He ages. Isotherms (dashed lines) are curved due to advection of mass and heat (red arrows) in the hanging wall and footwall, and topographic relief. Rocks in the subsurface (open circles) are exhumed to the surface (filled circles) by erosion. Laterally adjacent and underlying thrusts can complicate the cooling history of rocks.

range [34]. The lateral variation in exhumation rates and thermal gradients with distance from the fault influences rock cooling paths. He ages were calculated on these paths starting at 35 Ma (the assumed intrusion age) by holding the samples at their initial depth and temperature until exhumation initiated at 10 Ma. Fig. 5b shows predicted ages versus paleodepth. For paleodepths $< \sim 1.5$ km the ages decrease rapidly with paleodepth, just like the 0 mm/yr exhumation rate curve in Fig. 4. This represents the HePRZ developed between 35 and 10 Ma and now displaced to the surface by faulting and erosion. The steep part of the curve at depths $> 1.5$ km represents rocks that originated below the HePRZ that were rapidly exhumed. The 'break in slope' apparent in the plot at 10 Ma documents the onset of rapid exhumation. Below the break in slope the age–depth profile only crudely approximates the exhumation rate because rocks exhume at different rates and through different temperature gradients across the footwall. Numerical modeling can be used to translate this apparent rate into the true exhumation rate on the fault surface [11,38].

Fig. 5c shows the same predicted ages but plotted as a function of distance from the fault. The young ages between 0 and 25 km represent samples exhumed from below the HePRZ. The rapid increase in ages at distances $> 25$ km, well into the range, represent the exhumed HePRZ. The preservation of the HePRZ at greater distances from the fault reflects the smaller degrees of exhumation found close to the hinge line, and has been confirmed by several data sets [7,13].

### 3.3. Thrust fault settings

A rich body of literature exists concerning thermal processes that may influence cooling ages in thrust belts (e.g. [39–45]). Important factors may include (Fig. 6): (1) lateral heat flow across the fault from emplacement of a warm hanging wall over a cool footwall; (2) erosion of the hanging wall and sedimentation on the footwall; (3) thickening of radiogenic heat producing rocks; (4) displacement on adjacent or underlying thrust faults; (5) topography; and possibly (6) frictional heating on the fault. Here we discuss how the depth and shape of isotherms reflect the interplay of these processes and thus how He age patterns may vary in rocks exhumed in the hanging wall of a thrust fault.

Thrust fault processes that influence rock cooling are simplest in thick-skinned, basement-cored uplifts, where a master thrust typically accommo-

dates displacement, e.g. Laramide structures of Wyoming, and the Sierra Pampeannas of Argentina. In these environments hanging wall rocks cool in response to both structural and erosional cooling. Structural cooling refers to heat flow from a relatively warmer hanging wall to a cooler footwall. Unlike a normal fault, displacement on a thrust fault does not cause exhumation, and erosion is required to bring rocks to the surface (e.g. [46]). The distinction between structural and erosional cooling is important when interpreting He ages because erosion can be synchronous with or post-date thrust faulting and the exhumation pathway and cooling history of rocks towards the surface will depend on the timing, rate and magnitude of erosion (e.g. Fig. 6). Some modeling and dating studies have considered structural and erosional cooling in concert (e.g. [41,42,45]) by prescribing an erosion history. However, the relative significance of erosional versus structural cooling in a thrust environment has yet to be explored using physically based erosion models coupled with thermo-kinematic models of thrust emplacement. The apatite He technique provides renewed impetus for such work.

Cooling of rocks in thin-skinned fold and thrust belts is subject to the same processes as their thick-skinned counterparts, but can be complicated by other factors. Thin-skinned thrust environments are characterized by multiple thrust faults that accommodate up to hundreds of km of shortening and do not necessarily involve large amounts of basement uplift. Examples of this type of environment can be found in the Canadian Rocky Mountains, Taiwan, Zagros Mountains of Iran, and the Bolivian fold and thrust belt. Thin-skinned thrust belts have the additional complication of displacement on closely spaced adjacent (imbricate) thrusts, or underlying (duplex) structures influencing the cooling history (e.g. [40]). For example, in Fig. 6 displacement of the left hand thrust could influence the thermal field of the previously active right hand thrust by either lateral heat flow or by structural thickening of the right hand hanging wall, thereby enhancing relief and erosion. Additional complications associated with He dating in thin-skinned thrust belts can include insufficient exhumation to bring samples from closure temperature depths to the surface, and poor apatite grain quality associated with sedimentary rocks that commonly constitute such structures (unpublished data).

Important conclusions that could result from integrated He thermochronometry and modeling studies of thrust belts include: (1) what are the exhumation pathways of rocks, (2) when and at what rate does erosion occur on hanging walls, and (3) how does faulting on adjacent and underlying structures influence the cooling history of this low temperature thermochronometer?

## 4. Surface processes and apatite He ages

The temperature field of the uppermost crust is sensitive to overlying topography, so cooling trajectories of exhuming rocks will vary from point to point beneath topographic features. This suggests a fundamentally different approach for the application of cooling ages. Unlike the examples given above in which age variations resulted from spatial variability in exhumation rate, here age variations can be produced in a region experiencing uniform exhumation but beneath topography. The age distribution may thus be inverted for paleotopography and may provide important limits on paleoelevation. He ages are uniquely suited to this new approach (e.g. [19,47]).

### 4.1. *Topographic effects on subsurface temperatures*

The effect of topography on subsurface temperatures has long been known [48], and more recent studies have investigated how topography affects cooling histories using 2D thermal models [14,15,49,50]. These studies conclude that spatial and temporal variations in cooling rate depend on the wavelength and amplitude of the topography, as well as the exhumation rate and duration. The implications of topography for low temperature cooling ages in exhuming terrains is not generally appreciated, so we present an example of a He age pattern solely attributable to topographic control. Rather than a generic 2D representation of topography, we use as an example a 3D nu-

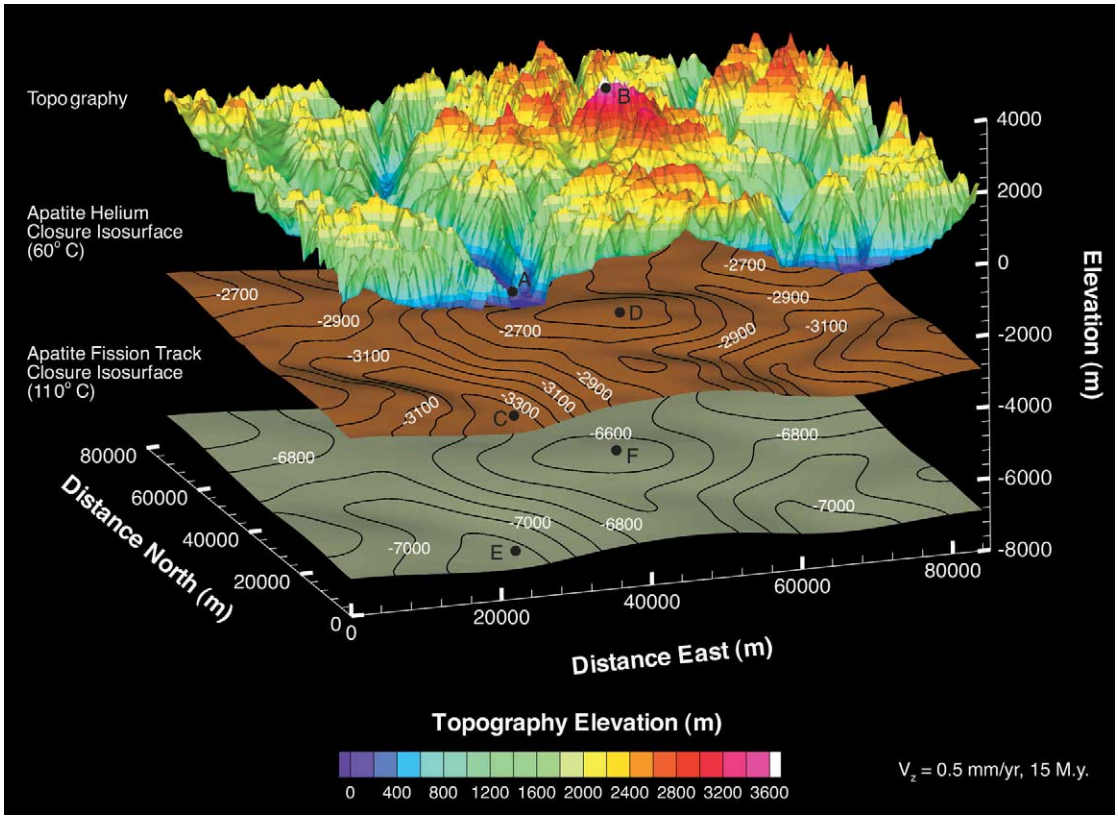


Fig. 7. Topographic effect on He and fission track closure temperature surfaces. Results are from a 3D transient thermal model (modified version of [51,52]) of Mt. Waddington, British Columbia. Model parameters include: basal heat flow boundary condition of 10 mW $m^{-2}$, zero flux boundary condition on the sides, constant surface temperature boundary condition with adiabatic lapse rate of 7°C/km, thermal conductivity of 2.7 W $m^{-1}$ $K^{-1}$, constant crustal heat production of 0.1 μW $m^{-3}$, crustal thickness of 35 km, average node spacing of 300 m, uniform exhumation rate of 0.5 mm/yr, and a simulation duration of 15 Myr. Initial condition is the steady-state solution for the prescribed boundary conditions with 0 mm/yr exhumation rate. Contour interval on depths to the closure surfaces (solid black lines) is 100 m. Fission track and He closure temperatures were computed by using the mean cooling rate of all samples exhumed to the surface after 15 Myr.

merical model of the region surrounding ~4 km high Mount Waddington, British Columbia (Fig. 7).

The model assumes steady-state topography and a uniform exhumation rate of 0.5 mm/yr, which corresponds to a closure temperature of 60°C [4]. Fig. 7 shows that the He closure temperature surface is a damped version of the topography, as predicted by 2D models [14]. However, the irregular morphology of the closure surface confirms the necessity of the 3D approach. The topographic relief between the valley floor and top of Mount Waddington (points A and B, respectively) is 3600 m, whereas the maximum relief on the He closure isotherm (points C and D) is about 900 m.

Topographic influence on temperatures decreases with depth, so the closure surface of a higher temperature thermochronometer will have less relief than the He closure surface. For example, the maximum relief on the apatite fission track closure surface (110°C, Fig. 7, points E and F) is ~500 m. At sufficiently large depths topographic perturbations to the thermal field are negligible and isotherms are flat-lying. Thus the apatite He system is uniquely sensitive to topographic perturbations to the temperature field.

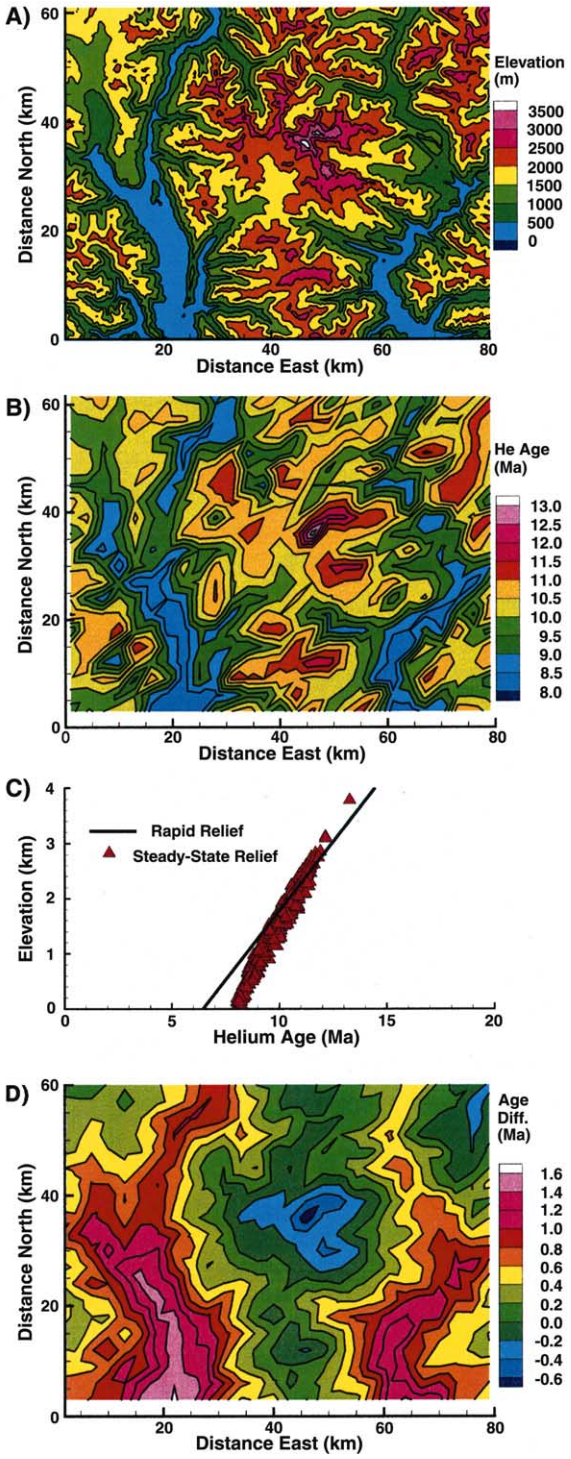


### 4.2. Measuring changes in topographic relief

Are He ages sufficiently sensitive and precise to document the existence of topography during exhumation? Several studies have approached this question using 2D numerical models [49,50] and He age patterns [6,47]. We address it by comparing He ages from two end-member scenarios that could produce the topography in Fig. 7: steady-state relief as described above, and recent instantaneous relief development of an initially flat surface (Fig. 8). For the case of instantaneous relief development rocks are exhumed through flat-lying isotherms towards a horizontal surface. Relief forms after rocks in the upper crust have closed to He loss. For the case of steady-state, relief is held fixed from the onset of exhumation, and isotherms are curved as in Fig. 7. These two models impose the maximum possible difference in thermal histories for rocks exposed on identical topographic surfaces.

In the case of steady-state relief He ages are predicted to range from 8 Ma in major valley bottoms (fjords) to 13 Ma at the top of the highest peak (Fig. 8a,b). Predicted ages for the rapid relief development model were computed assuming the same exhumation rate of 0.5 mm/yr, and the mean geothermal gradient from the steady-state model (Fig. 7). In an age–elevation plot (Fig. 8c) this model defines a straight line of slope 0.5 mm/yr, just as in the 1D models of Fig. 4. In contrast, the steady-state model yields a steeper profile with a slope of 0.8 mm/yr (triangles, Fig. 8c). The higher slope is qualitatively consistent with 2D thermal models that show 1D interpretations overestimate the exhumation rate in areas of high relief [15]. The simple explanation for this

←

Fig. 8. Predicted He ages for end-member models of rapid and steady-state relief development, Coast Mountains, British Columbia. (A) Topography of the Coast Mountains. (B) Predicted He ages for the steady-state relief model using the 3D model result in Fig. 7. Ages were predicted on a grid of points spaced 3 km across the topography. (C) Predicted He ages for the rapid relief development model (solid line) and steady-state relief model (triangles). (D) Difference in predicted He ages between the steady-state relief and rapid relief development models. See text for discussion.

overestimation is that rocks from low elevations come from valleys beneath which the closure isotherm is closer to the surface, while, in contrast, high elevation samples come from topographic highs beneath which the closure isotherm is at greater depths (Fig. 7).

The relationship between topography and the difference between ages predicted by the two models is evident in map view (Fig. 8e). At higher elevations of the main massif the 3D ages are up to 0.6 Ma younger than the 1D ages, while in the fjords they are up to 1.6 Ma older. This difference is sufficiently large to be detected: at the $\sim$8 Ma ages in these simulations, 2$\sigma$ age uncertainties are likely to be $<$0.5 Ma. Put differently, the steady-state relief model predicts readily detectable spatial variability in ages, correlated with topography but in the absence of spatial variability in exhumation rate. Thus He ages can document the existence of paleotopography, as has been seen in the Sierra Nevada [6,47]. Similarly, helium thermochronometry has the ability to detect a change in relief after exhumation, e.g. resulting from Pleistocene glaciation. Other surface process applications include quantifying rates of river incision or large scale changes in relief between valleys [49,50].

## 5. Future directions of apatite He thermochronometry

Apatite He thermochronometry is still in its first decade of development so key issues warrant continued attention.

### 5.1. Methodological considerations

We need a better understanding of what controls He diffusivity in apatite, ideally related to readily measurable quantities. Our present knowledge is based on sparse observations and remains completely empirical. To take full advantage of the precision of the method we also require more accurate He diffusivity estimates. Looking further, linking of He thermochronometry with other low temperature systems, such as apatite fission track ages and length models and K-feldspar multi-diffusion domain models, will provide a powerful tool for studying the transient exhumation rates in the upper crust. However, this application requires rigorous intercalibration of the thermal sensitivities of these methods, which is only just beginning [13].

### 5.2. Applications

Rocks cool as a result of structural processes (e.g. faulting, underplating) and by erosion. Most studies to date focus on either the tectonic or surface processes that result in cooling but do not consider both processes in concert. Apatite (U–Th)/He dating integrated with coupled thermo-tectonic-erosion models provides a quantification of the interaction between tectonics and erosion in landscape evolution. Integrating data with numerical models will allow us to link the longer-term tectonic processes with shorter-term geomorphic processes. There are many important problems which can be addressed by the quantification made possible with this technique.

## Acknowledgements

This research was funded by the National Science Foundation. Margie Rusmore and Glenn Woodsworth are thanked for thoughtful discussions about Coast Mountains, BC geology. Digital elevation models used in Figures 7 and 8 were provided through collaboration with G. Woodsworth and the Canadian Geologic Survey. We acknowledge Simon P. Kelley and Urs Schaltegger for constructive reviews.*[AH]*

## References

[1] P.K. Zeitler, A.L. Herczig, I. McDougall, M. Honda, U-Th-He dating of apatite: a potential thermochronometer, Geochim. Cosmochim. Acta 51 (1987) 2865–2868.
[2] H.J. Lippolt, M. Leitz, R.S. Wernicke, B. Hagedorn, (U+Th)/He dating of apatite experience with samples from different geochemical environments, Chem. Geol. 112 (1994) 179–191.
[3] R.A. Wolf, K.A. Farley, L.T. Silver, Helium diffusion and low temperature thermochronometry of apatite, Geochim. Cosmochim. Acta 60 (1996) 4231–4240.

[4] K.A. Farley, Helium diffusion from apatite: general behavior as illustrated by Durango fluorapatite, J. Geophys. Res. 105 (2000) 2903–2914.
[5] K.A. Farley, (U-Th)/He dating: Techniques, calibrations, and applications, in: P.D. Porcelli, C.J. Ballentine, R. Wieler (Eds.), Noble Gas Geochemistry, Reviews in Mineralogy and Geochemistry vol. 47 (2002), pp. 819–843.
[6] M.A. House, B.P. Wernicke, K.A. Farley, Dating topography of the Sierra Nevada, California, using apatite (U-Th)/He ages, Nature 396 (1998) 66–69.
[7] D.F. Stockli, K.A. Farley, T.A. Dumitru, Calibration of the (U-Th)/He thermochronometer on an exhumed fault block, White Mountains, California, Geology 28 (2000) 983–986.
[8] K.A. Farley, M.E. Rusmore, S.W. Bogue, Post-10 Ma uplift and exhumation of the Northern Coast Mountains, British Columbia, Geology 29 (2001) 99–102.
[9] R.A. Wolf, K.A. Farley, L.T. Silver, Helium diffusion and low temperature thermochronometry of apatite, Geochim. Cosmochim. Acta 60 (1996) 4231–4240.
[10] R.A. Ketcham, D.A. Donelick, W.D. Carlson, Variability of apatite fission-track annealing kinetics: III. Extrapolation to geologic time scales, Am. Mineral. 84 (1999) 1235–1255.
[11] T.A. Ehlers, S.D. Willett, P.A. Armstrong, D.S. Chapman, Exhumation of the central Wasatch Mountains, Utah: 2. Thermo-kinematic model of exhumation, erosion, and thermochronometer interpretation, J. Geophys. Res. (2002) in press.
[12] G.E. Batt, M.T. Brandon, K.A. Farley, M. Roden-Tice, Tectonic synthesis of the Olympic Mountains segment of the Cascadia wedge, using two-dimensional thermal and kinematic modeling of thermochronological ages, J. Geophys. Res. 106 (2001) 26731–26746.
[13] P.A. Armstrong, T.A. Ehlers, D.S. Chapman, K.A. Farley, P.J.J. Kamp, Exhumation of the central Wasatch Mountains, Utah: 1. Patterns and timing deduced from low-temperature thermochronology data, J. Geophys. Res. (2002) in press.
[14] K. Stuwe, L. White, R. Brown, The influence of eroding topography on steady-state isotherms - application to fission track analysis, Earth Planet. Sci. Lett. 124 (1994) 63–74.
[15] N.S. Mancktelow, B. Grasemann, Time-dependent effects of heat advection and topography on cooling histories during erosion, Tectonophysics 270 (1997) 167–195.
[16] D. Stockli, J. Linn, J.D. Walker, T. Dumitru, Miocene unroofing of the Canyon Range during extension along the Sevier Desert Detachment, west central Utah, Tectonics 20 (2001) 289–307.
[17] K.A. Farley, B.P. Kohn, B. Pillans, (U-Th)/He dating of Pleistocene zircon and apatite: A test case from the Rangitawa tephra, North Island, New Zealand, Earth Planet. Sci. Lett. 201 (2002) pp. 117–125.
[18] K. Min, K.A. Farley, P.R. Renne, K. Marti, Single grain (U-Th)/He ages from phosphates in Acapulco meteorite and implications for thermal history, Earth Planet. Sci. Lett. (2002).
[19] C. Persano, F. Stuart, P. Bishop, D. Barfod, Apatite (U-Th)/He age constraints on the development of the Great Escarpment on the southeastern Australian passive margin, Earth Planet. Sci. Lett. 200 (2002) 79–90.
[20] M. House, K. Farley, D. Stockli, Helium chronometry of apatite and titanite using Nd-YAG laser heating, Earth Planet. Sci. Lett. 183 (2000) 365–368.
[21] P.W. Reiners, T.A. Ehlers, J.I. Garver, S.G. Mitchell, D.R. Montgomery, J.A. Vance, S. Nicolescu, Late Miocence exhumation and uplift of the Washington Cascades, Geology 30 (2002) 767–770.
[22] M.A. House, B.P. Wernicke, K.A. Farley, T.A. Dumitru, Cenozoic thermal evolution of the central Sierra Nevada from (U-Th)/He thermochronometry, Earth Planet. Sci. Lett. 151 (1997) 167–179.
[23] B.I.A. McInnes, K.A. Farley, R.H. Sillitoe, B.P. Kohn, Application of apatite (U-Th)/He thermochronometry to the determination of the sense and amount of vertical fault displacement at the Chuqicamata porphyry copper deposit, Chile, Econ. Geol. 94 (1999) 937–947.
[24] K.A. Farley, R.A. Wolf, L.T. Silver, The effects of long alpha-stopping distances on (U-Th)/He ages, Geochim. Cosmochim. Acta 60 (1996) 4223–4229.
[25] A.G.C.A. Meesters, T.J. Dunai, Solving the production-diffusion equation for finite diffusion domains of various shapes: Part II. Application to cases with α-ejection and non-homogeneous distribution of the source, Chem. Geol. 186 (2002) 57–73.
[26] A.C. Warnock, P.K. Zeitler, R.A. Wolf, S.C. Bergman, An evaluation of low-temperature apatite U-Th/He thermochronometry, Geochim. Cosmochim. Acta 61 (1997) 5371–5377.
[27] H. Fechtig, S. Kalbitzer, The diffusion of argon in potassium bearing solids, in: O.A. Schaeffer, J. Zahringer (Eds.), Potassium-Argon Dating, Springer, Heidelberg, 1966, pp. 68–106.
[28] M.H. Dodson, Closure temperatures in cooling geological and petrological systems, Contrib. Mineral. Petrol. 40 (1973) 259–274.
[29] M.A. House, K.A. Farley, B.P. Kohn, An empirical test of helium diffusion in apatite: borehole data from the Otway basin, Australia, Earth Planet. Sci. Lett. 170 (1999) 463–474.
[30] P.W. Reiners, K.A. Farley, Influence of crystal size on apatite (U-Th)/He thermochronology: an example from the Bighorn mountains, Wyoming, Earth. Planet. Sci. Lett. 188 (2001) 413–420.
[31] R.A. Wolf, K.A. Farley, D.M. Kass, A sensitivity analysis of the apatite (U-Th)/He thermochronometer, Chem. Geol. 148 (1998) 105–114.
[32] P.W. Reiners, R. Brady, K.A. Farley, J. Fryxell, B. Wernicke, D. Lux, Helium and argon thermochronometry of the Gold Butte Block, south Virgin Mountains, Nevada, Earth Planet. Sci. Lett. 178 (2001) 315–326.
[33] A.E. Benfield, The effect of uplift and denudation on

underground temperatures, J. Appl. Phys. 20 (1949) 66–70.
[34] T.A. Ehlers, D.S. Chapman, Normal fault thermal regimes conductive and hydrothermal heat transfer surrounding the Wasatch fault, Utah, Tectonophysics 312 (1999) 217–234.
[35] J.D. van Wees, K. de Jong, S. Cloetingh, Two-dimensional P-T-t modelling and the dynamics of extension and inversion in the Betic Zone (SE Spain), Tectonophysics 203 (1992) 305–324.
[36] B. Grasemann, N.S. Mancktelow, Two-dimensional thermal modelling of normal faulting the Simplon Fault Zone, central Alps, Switzerland, Tectonophysics 225 (1993) 155–165.
[37] M. ter Voorde, G. Bertotti, Thermal effects of normal faulting during rifted basin formation. 1. A finite difference model, Tectonophysics 240 (1994) 133–144.
[38] T.A. Ehlers, P.A. Armstrong, D.S. Chapman, Normal fault thermal regimes and the interpretation of low-temperature thermochronometers, Phys. Earth Planet. Inter. 126 (2001) 179–194.
[39] J. Brewer, Thermal effects of thrust faulting, Earth Planet. Sci. Lett. 56 (1981) 233–244.
[40] P. Davy, P. Gillett, The stacking of thrust slices in collision zones and its thermal consequences, Tectonics 5 (1986) 913–929.
[41] D. Maihe, F. Lucazeau, G. Vasseur, Uplift history of thrust belts: An approach based on fission track data and thermal modelization, Tectonophysics 124 (1986) 177–191.
[42] Y. Shi, C. Wang, Two-dimensional modeling of the P-T-t paths of regional metamorphism in simple overthrust terrains, Geology 15 (1987) 1048–1051.
[43] P. Karabinos, R. Ketcham, Thermal structure of active thrust belts, J. Metamorph. Geol. 6 (1988) 559–570.
[44] C. Ruppel, K.V. Hodges, Role of horizontal thermal conduction and finite time thrust emplacement in simulation of pressure-temperature-time paths, Earth Planet. Sci. Lett. 123 (1994) 49–60.
[45] M.K. Rahn, B. Grasemann, Fission track and numerical thermal modeling of differential exhumation of the Glarus thrust plan (Switzerland), Earth Planet. Sci. Lett. 169 (1999) 245–259.
[46] U. Ring, M.T. Brandon, S.D. Willett, G.S. Lister, Exhumation processes, in: U. Ring, M.T. Brandon, G.S. Lister, S.D. Willett (Eds.), Exhumation Processes: Normal Faulting, Ductile Flow, and Erosion, Geol. Soc. London Spec. Publ. 154, 1999, pp. 1–27.
[47] M.A. House, B.P. Wernicke, K.A. Farley, Paleo-geomorphology of the Sierra Nevada, California, from (U-Th)/He ages in apatite, Am. J. Sci. 301 (2001) 77–102.
[48] C.H. Lees, On the isogeotherms under mountain ranges in radioactive districts, Proc. R. Soc. 83 (1910) 339–346.
[49] K. Stuwe, M. Hintermueller, Topography and isotherms revisited: the influence of laterally migrating drainage divides, Earth Planet. Sci. Lett. 184 (2000) 287–303.
[50] J. Braun, Quantifying the effect of recent relief changes on age-elevation relationships, Earth Planet. Sci. Lett. 200 (2002) 331–343.
[51] T. Kohl, R.J. Hopkirk, 'FRACTure': a simulation code for forced fluid flow and transport in fractured, porous rock, Geothermics 24 (1995) 333–343.
[52] T. Kohl, Transient thermal effects below complex topographies, Tectonophysics 306 (1999) 311–324.

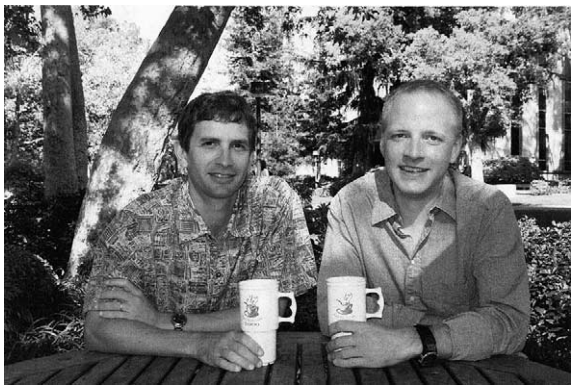

T.A. Ehlers (right) is a geodynamicist at the University of Michigan whose main research emphasis is the interactions between climate, tectonics, and topography and their respective roles in landform evolution. His research integrates thermochronometer and exposure-age data with coupled thermal, kinematic, atmospheric, and surface-process numerical models. K.A. Farley (left) is a geochemist at the California Institute of Technology with a primary interest in the development of techniques and applications of noble gas geochemistry. Recent interests include geochronology and exposure-age dating, the geochemical evolution of the mantle, and the depositional history of interplanetary dust.